**EVIDENCE FOR RAPID GROWTH OF MELILITE IN AN UNUSUAL COMPACT TYPE A REFRACTORY INCLUSION FROM ALLENDE**. S. B. Simon[1], A. M. Davis[2], and L. Grossman[1,2], [1]Dept. of the Geophysical Sciences, 5734 S. Ellis Ave., [2]Enrico Fermi Institute, University of Chicago, Chicago, IL 60637.

Compact Type A (CTA) inclusions are extremely melilite-rich (typically ~90 vol%), with moderate amounts of spinel and minor fassaite and perovskite. Because CTAs are one of the major types of coarse-grained inclusions found in CV3 chondrites but have not been thoroughly studied as a group, we have undertaken a comprehensive petrographic, mineral-chemical, and trace element study of a large suite of CTAs from the CV3 chondrites Allende, Axtell, Efremovka, and Leoville. A preliminary report of our results for some representative members of the suite was given by [1]. Here we report the results of a detailed study of a unique member of the suite, Allende inclusion TS2.

**Petrography and mineral chemistry.** TS2 is round in cross-section and 5.2 mm in diameter. It is dominated by very large (0.1–2 mm) melilite crystals and, as noted by [2], chains and clusters of coarse (50–150 μm) spinel grains, with ~1 vol% each of perovskite and fassaite. Digital X-ray mapping of the entire inclusion shows that melilite in the outer ~500 μm of the inclusion tends to be more aluminous ($Åk_{15–50}$) than that in the interior ($Åk_{30–70}$). A distinctive, major feature of this inclusion is that many melilite crystals have no dominant core-rim zoning but instead consist of 50–200 μm patches of aluminous melilite ($Åk_{25–53}$, median $Åk_{38}$, with a normal distribution of compositions) (Fig. 1) set in, and optically continuous with, relatively Mg-rich melilite ($Åk_{32–62}$, median $Åk_{51}$, with a distribution that is skewed towards aluminous melilite) (Fig. 2). Within many individual crystals, especially in the interior of the inclusion, the aluminous patches enclose numerous 0.5–5 μm spinel grains while the relatively Åk-rich patches are either spinel-free or adjacent to coarse spinel. The spinel-bearing, Åk-poor melilite is never in contact with melilite grain boundaries. Toward the edge of the inclusion (the outer ~500 μm), Åk-poor patches are not associated with fine-grained spinel.

The distributions of coarse and fine spinel are quite different. Coarse spinel occurs in clumps and chains, whereas the fine spinel grains are never clumped together. Both rastered beam X-ray microanalysis and digital analysis of backscattered electron images show that there is about 5 vol% spinel, 1 vol% fassaite, and 0.05 vol% perovskite in the spinel-bearing Åk-poor zones. Both the coarse and fine spinel have 0.2–0.4 wt% $Cr_2O_3$ and 0.4–0.7 wt% $TiO_2$. The fine spinel has lower $V_2O_3$ contents than the coarse spinel (~0.3 vs. 0.3–0.6 wt%). The coarse spinels are unzoned. Both the bimodal size distribution of spinel and the patchy zoning of melilite are unique to this inclusion. Mapping also reveals that one of the curved chains of coarse spinel marks the boundary of a spinel-free palisade body, 1.7×0.85 mm, that consists of relatively Åk-rich (45–65 mol%) melilite and minor perovskite. Several melilite crystals adjacent to the spinel wall are oriented radially and may have grown inward from it. An electron probe traverse along the length of one such grain shows that, with increasing distance from the spinel wall, its Åk content drops from 49 to 44 mol% over the first 10 μm and then increases to 62 mol% over the remaining 250 μm of the crystal, with several narrow (10–20 μm) bands of reverse zoning. In this crystal, $Na_2O$ contents are positively correlated with Åk contents, a relationship expected for igneous melilite [3] but not apparent in the patchy melilite. The palisade body also contains two grains of unusual, Nb-rich (~4–6 wt% $Nb_2O_5$) perovskite enclosed in "normal", Nb-poor perovskite.

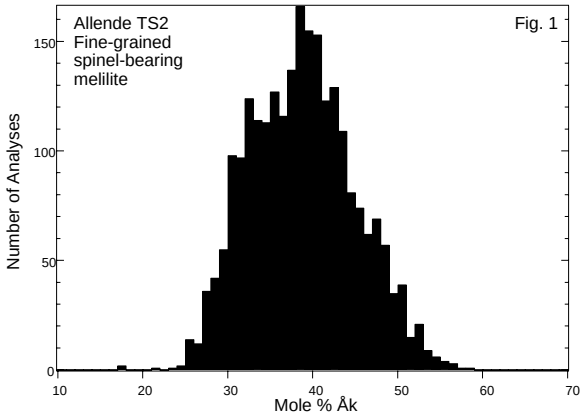


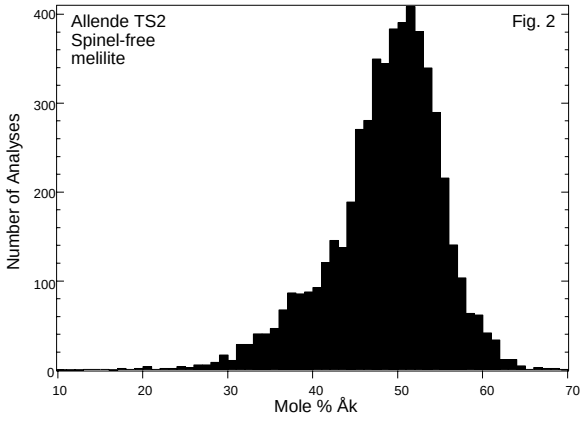


**Trace elements.** Ion microprobe analysis of perovskite, fassaite, and melilite from all three petrographic regimes (patchy melilite associated with fine spinel; patchy melilite not associated with spinel; and the palisade body) shows that the bulk CAI has a REE pattern closely related to the Group II patterns commonly found in fine-grained CAIs in Allende. This pattern, in which the refractory heavy REE are strongly depleted relative to the other REE, is relatively rare among coarse-grained inclusions. The REE pattern dif-

fers from normal Group II patterns in that Eu and Yb have the same enrichment factor as LREE rather than being depleted. All phases in this inclusion show this Group II-like REE pattern overprinted on REE fractionations consistent with crystal/melt partition coefficients, regardless of location within the CAI. Like melilite from Type B1 inclusions [4], plots of trivalent REE abundances vs. Åk show considerable scatter, largely because most analysis spots contain tiny inclusions of fassaite and/or perovskite. Ten (out of 30) analysis spots that are apparently free of such inclusions show a steady decrease of La, Yb and Yb/La with increasing Åk. This relationship is similar to that in Type B1 CAIs, which are believed to have crystallized from melts [4]. Sr abundances are also positively correlated with Åk and are consistent with crystallization of melilite from a liquid with a bulk Sr content of 33×C1 chondrites, assuming a crystal/liquid D of 0.8 [5].

The slopes of REE patterns in perovskite increase, becoming more LREE-enriched, with increasing overall REE content. On a plot of Nb vs. La, two compatible elements, analyses of perovskite from the palisade body and throughout the inclusion fall on a single linear trend with a positive slope. Both of these features are consistent with crystallization of perovskite from a late-stage melt. Fassaite shows negative correlations between REE and Sc, which is consistent with fractional crystallization [6]. The ion probe results indicate that all the components of this inclusion formed from the same source, and the trace element variations within each phase are consistent with crystallization from a melt.

**Discussion.** This inclusion is unusual in terms of its texture (patchy melilite, bimodal spinel sizes), mineral chemistry (almost all melilite is more Mg-rich than $Åk_{30}$, whereas $Åk_{<30}$ is typical of CTAs), and bulk composition (Group II pattern, 10.3 wt% MgO [7]). If we assume that the Group II REE patterns, found in minerals throughout the inclusion, mean that all the grains crystallized from the same melt, then the unusual texture must reflect an unusual thermal history rather than incorporation of xenoliths or additional liquids.

The morphology of, and numerous spinel inclusions in, the Åk-poor cores of interior melilite crystals are suggestive of rapid cooling. It is not clear whether the spinel, fassaite and perovskite inclusions represent tiny crystals trapped during rapid growth of melilite, or are exsolution products from rapidly crystallized, nonstoichiometric melilite. The latter possibility is suggested by two observations: (1) the fine grains of spinel are dispersed rather than occurring in clumps or chains; (2) the presence of tiny inclusions of fassaite and perovskite, phases that normally crystallize very late from melts of the composition of TS2 and would not be expected to be found included in early melilite. Two arguments against exsolution are that considerable nonstoichiometry of melilite is required (the spinel-bearing melilite areas contain ~5% spinel), and a lack of previous reports of nonstoichiometric melilite, even in experimental run products cooled at 1000˚C/hr [8].

The following petrologic history best accounts for the observations. (1) Precursors that have a Group II REE pattern melt. (2) Bubbles form in melt and become lined with spinel [9], forming spinel chains. (3) Rapid growth of large, dendritic melilite crystals occurs, due to rapid cooling or perhaps due to supercooling, leading to crystallization of nonstoichiometric melilite enriched in spinel components and excess Ti, and trapping of melt. (4) After growth of dendritic melilite, more Åk-rich melilite and coarse spinel grow at a slower rate consistent with a moderate cooling rate of a few degrees per hour; bubbles coalesce, break, and fill with fractionated melt [9], which crystallizes to Åk-rich melilite±fassaite, ±perovskite, as does melt that was trapped in early melilite. The late melilite takes on the same optical orientation as the substrate melilite.

There are several ways in which the observations are consistent with an early episode of rapid cooling. Experiments [8,10,11] show that at cooling rates >50˚C/hr or at $T_{max}$ >1500˚C, melilite commonly crystallizes as coarse, dendritic crystals, with pockets of melt between the branches and enclosed in the crystals. Trapping of evolved melt followed by devitrification of glass or crystallization of overgrowths on the host could give rise to patchy zoning of melilite. Experiments [8,11] also show that as cooling rate increases, the onset of melilite crystallization is suppressed, so that the earliest melilite in rapidly cooled runs tends to have higher Åk contents than that in slowly ($\leq$ 5˚C/hr) cooled runs. This, along with its Mg-rich bulk composition, may explain why the melilite in TS2 is more Åk-rich than that in most CTAs. Finally, some experiments [8] on CAI melts cooled at 200˚C/hr yielded two generations of spinel, one early and coarse (100-200 μm) occurring around the edge of the charge, the other relatively late and fine ( < 25 μm) and concentrated in the interior. While this result does not account for the spatial distribution of spinel in TS2, it does suggest a possible link between the bimodal size distribution of spinel in TS2 and a rapid cooling rate. We cannot rule out, however, the possibility that the rapid growth of the spinel-bearing, Åk-poor melilite in TS2 was due to substantial undercooling prior to melilite nucleation.

**References.** [1] Simon S. B. et al. (1995) *LPS* **26**, 1303. [2] Grossman L. (1975) *GCA* **39**, 433. [3] Beckett J. R. and Stolper E. (1994) *LPS* **25**, 79. [4] Davis A. M. et al. (1992) *LPS* **23**, 281. [5] Beckett J. R. et al. (1990) *GCA* **54**, 1755. [6] Simon S. B. et al. (1991) *GCA* **55**, 2635. [7] Beckett J. R. (1986) Ph.D. Diss., U. of Chicago. [8] Stolper E. & Paque J. M. (1986) *GCA* **50**, 1785. [9] Simon S. B. & Grossman L. (1997) *Meteoritics & Planet. Sci*. **32**, in press. [10] Paque J. M. & Stolper E. (1984*) LPS* **25**, 631. [11] Simon S. B. et al. (1996) *LPS* **27**, 1201.